

Mesic nuclei with a heavy antiquark

Yasuhiro Yamaguchi

*E-mail: yasuhiro.yamaguchi@ge.infn.it

*Istituto Nazionale di Fisica Nucleare (INFN), Sezione di Genova, via
Dodecaneso 33, 16146 Genova, Italy,*

*Theoretical Research Division, Nishina Center, RIKEN, Wako, Saitama
351-0198, Japan*

and

Shigehiro Yasui

*Department of Physics, Tokyo Institute of Technology, Tokyo 152-8551,
Japan*

.....
The binding of a hadron and a nucleus is a topic of great interest for investigating the hadron properties. In the heavy-flavor region, attraction between a $P(= \bar{D}, B)$ meson and a nucleon N can appear, where $PN - P^*N$ mixing plays an important role in relation to the heavy-quark spin symmetry. The attraction can produce exotic heavy mesic nuclei that are stable against strong decay. We study an exotic system where the \bar{D} (B) meson and nucleus are bound. The meson-nucleus interaction is given by a folding potential with single-channel PN interaction and the nucleon number distribution function. By solving the Schrödinger equations of the heavy meson and the nucleus, we obtain several bound and resonant states for nucleon number $A = 16, \dots, 208$. The results indicate the possible existence of exotic mesic nuclei with a heavy antiquark.
.....

Subject Index D06, D15

1 Introduction

Multiflavor nuclei are interesting objects for studying unconventional states of matter in the hadron and nuclear physics. As a first step towards extending the quark flavor, strangeness nuclei have been extensively studied both in experiments and in theories. As a new direction, charm and bottom are new flavors whose properties in nuclei should be different from those of strangeness nuclei [1]. Charm/bottom nuclei, as well as strangeness nuclei, are important for studying (i) the heavy hadron and nucleon interaction, (ii) the properties of heavy hadrons in a nuclear medium, and (iii) the impurity effect for nuclear properties. These are related to the flavor symmetry of the interhadron interaction, the partial restoration of the broken chiral symmetry, and so on, as fundamental problems in quantum chromodynamics (QCD). In theoretical studies, there has been a lot of research into heavy baryons, heavy mesons and quarkonia in nuclear systems (see Ref. [1] and references therein). Recently, few-body calculations have also been performed [2–5]. In the present study, we focus on the properties of the \bar{D} (B) mesons with a quark content $\bar{Q}q$ with a heavy antiquark \bar{Q} and a light quark q , which can be bound in finite-size atomic nuclei.

The \bar{D} (B) meson in nuclear systems is a simple system, because there is no annihilation channel by $\bar{q}q$, in contrast to the case of its antiparticle D (\bar{B}) in nuclear medium. They have both been studied in many theoretical works: the quark-meson coupling model [6, 7], the mean-field approach [8–11], the flavor SU(4) symmetry [12–15], the flavor-spin SU(8) symmetry [16], the pion-exchange interaction [17, 18], the QCD sum rules [19–24], and the Nambu–Jona-Lasinio model [25]. As advanced topics, there are studies on chiral symmetry breaking [26–29], the Kondo effect [30–32]¹, and the spin-isospin correlated nuclear matter [38]. Few-body calculations of $\bar{D}NN - \bar{D}^*NN$ ($BNN - B^*NN$) have also been performed [4]. The interaction between a \bar{D} (B) meson and a nucleon can be provided by the meson exchange interaction. At short distances, it is supplied by the exchange of heavy mesons (e.g., scalar mesons and vector mesons) and by the direct exchange of quarks [39–43]. At long distances, pion exchange can occur, because the pion is the lightest meson as the Nambu-Goldstone bosons generated by the dynamical breaking of chiral symmetry in vacuum [41–47].

The symmetry that governs the \bar{D} (B) meson dynamics is given by the heavy-quark (spin) symmetry (HQS) for the heavy-antiquark component and chiral symmetry for the light-quark component [48–50]. One of the most important properties of the HQS is that the

¹The Kondo effect is also considered in quark matter, where the color degrees of freedom play an essential role [33–37].

spin degree of freedom of a heavy (anti)quark is decoupled from the spatial rotation. Then, the heavy-quark spin is independent of the light spin j , which is carried by light quarks and gluons, as a sum of angular momenta and intrinsic spins. As a consequence, there exist two different types of heavy hadron states: the HQS singlet ($j = 0$) and the HQS doublet ($j \geq 1/2$) [48–52]. A \bar{D} (B) meson is regarded approximately as an HQS doublet whose pairs are given by a \bar{D}^* (B^*) meson, because the mass difference is of the order of $1/m_c$ ($1/m_b$) with m_c (m_b) being the charm (bottom) quark mass. This is a good approximation because the charm (bottom) quark mass is larger than the typical low-energy scale of the hadron dynamics, say a few hundred MeV, and they can be regarded as being sufficiently heavy. One of the interesting results of the HQS is that the mixing of a \bar{D} (B) meson and a \bar{D}^* (B^*) meson is realized in nuclear medium via the interaction process $\bar{D}N \leftrightarrow \bar{D}^*N$ ($BN \leftrightarrow B^*N$). This mixing leads to an attraction of the heavy-light hadrons in nuclear matter ².

The current status of theoretical studies, however, is that there are many open problems about the properties of the \bar{D} (B) meson and the \bar{D}^* (B^*) meson in nuclear systems. For example, the value of the binding energy of the \bar{D} (B) meson and/or the \bar{D}^* (B^*) meson in nuclear matter with infinite volume is not yet convergent. The values are highly scattered from a few MeV to a hundred MeV depending on the model used in the analysis. Hence more theoretical effort is needed to understand heavy hadrons in nuclear medium.

The purpose of the present study is to investigate the bound and/or resonant states of the \bar{D} (B) meson in atomic nuclei with finite nucleon numbers. As an interaction between a \bar{D} (B) meson and a nucleon, we adopt the pion exchange potential at long distances and the vector-meson exchange potential at short distances. The existence of the pion exchange interaction is an important result of the HQS, because the mixing process $\bar{D}N \leftrightarrow \bar{D}^*N$ ($BN \leftrightarrow B^*N$) plays an important role [45–47]. At first sight, there seems to be no $\bar{D}\bar{D}\pi$ ($BB\pi$) vertex by parity conservation, and hence there should be no pion exchange interaction for $\bar{D}N$ (BN). The pion exchange interaction for $\bar{D}N$ (BN) is indeed induced by the two-step process $\bar{D}N \rightarrow \bar{D}^*N \rightarrow \bar{D}N$ ($BN \rightarrow B^*N \rightarrow BN$). This mixing is available when the mass of a \bar{D}^* (B^*) meson is sufficiently close to the mass of a \bar{D} (B) meson, as expected from the (approximate) mass degeneracy in the heavy-quark limit. In this framework, we eliminate the dynamical degrees of freedom by a \bar{D}^* (B^*) meson in a systematic way, and obtain the effective interaction between a \bar{D} (B) meson and a nucleon. We then apply the

² This is a two-body mixing for spin degrees of freedom. An analogous process is seen in hypernuclei, i.e., $\Lambda N \leftrightarrow \Sigma N$ for isospin mixing. When the spin-isospin correlation exists in nuclear matter, one-body mixing by $\bar{D} \leftrightarrow \bar{D}^*$ ($B \leftrightarrow B^*$) can exist [38].

obtained $\bar{D}N$ (BN) potential to the calculation of the energy levels of a \bar{D} (B) meson in finite-size atomic nuclei.

This paper is organized as follows. In Sect. 2, we formulate the meson exchange potential between a heavy meson and a nucleon, perform the projection of the meson exchange potential, and give the meson-nucleus folding potential. In Sect. 3, we show the numerical results of the bound and resonant states. The last section is devoted to a summary.

2 Interactions between the heavy meson and the nucleus

The heavy meson in a nucleus is regarded as a two-body system of the meson and the nucleus. The meson-nucleus interaction is described as the folding potential, which can be obtained by the P meson-nucleon (PN) interaction and the nucleon number distribution function in the nucleus. Hereafter, we will use the notation P to stand for a \bar{D} meson or a B meson. We will also use the notation P^* for a \bar{D}^* meson or a B^* meson. As for the PN potential, we employ the meson exchange potential of the coupled-channel $PN - P^*N$, as discussed in Refs. [45–47]. The most simple $P^{(*)}N$ system is the S -wave state with the total spin $J = 1/2$. In Refs. [45–47], we found one bound state for $I = 0$, and no bound state for $I = 1$. Therefore, the $I(J^P) = 0(1/2^-)$ state is the most important one in the mesic nuclear system.

The $I(J^P) = 0(1/2^-)$ state has three channels, namely $PN(^2S_{1/2})$, $P^*N(^2S_{1/2})$ and $P^*N(^4D_{1/2})$, where the notation $^{2S+1}L_J$ is used to stand for the intrinsic total spin S , the angular momentum L and the total spin J . This potential is given by the 3×3 matrix form. We will project this potential onto the $PN(^2S_{1/2})$ channel, and use the single-channel PN potential to construct the folding potential.

2.1 Meson exchange potentials of $P^{(*)}$ meson and nucleon N

First of all, we introduce the meson exchange potential between a $P^{(*)}$ meson and a nucleon N . This potential is obtained by the effective Lagrangians of heavy mesons, light mesons, and nucleons, as discussed in Refs. [45–47].

The Lagrangians of heavy mesons and light mesons (pion and vector mesons), satisfying the heavy quark and chiral symmetries [53–55] (see also Refs. [48–50]), are employed in this study. Their interaction forms are given by

$$\mathcal{L}_{\pi HH} = ig_{\pi} \text{Tr} [H_b \gamma_{\mu} \gamma_5 A_{ba}^{\mu} \bar{H}_a], \quad (1)$$

$$\mathcal{L}_{v HH} = -i\beta \text{Tr} [H_b v^{\mu} (\rho_{\mu})_{ba} \bar{H}_a] + i\lambda \text{Tr} [H_b \sigma^{\mu\nu} F_{\mu\nu}(\rho)_{ba} \bar{H}_a]. \quad (2)$$

The subscripts π and v stand for the pion and vector mesons (ρ and ω), respectively. v^μ is the four-velocity of a heavy quark ($v^\mu v_\mu = 1$ and $v^0 > 0$). The subscripts a, b are for light flavor (u, d). The heavy-meson fields H_a are given by

$$H_a = \frac{1 + \psi}{2} [P_{a\mu}^* \gamma^\mu - P_a \gamma_5], \quad \bar{H}_a = \gamma_0 H_a^\dagger \gamma_0, \quad (3)$$

where $P_{a\mu}^*$ and P_a are the fields of P^* and P mesons, respectively, with light flavor a . A^μ is the axial current of a pion, expressed as

$$A^\mu = \frac{1}{2} (\xi^\dagger \partial^\mu \xi - \xi \partial^\mu \xi^\dagger), \quad (4)$$

with $\xi = \exp(i\hat{\pi}/f_\pi)$, the pion decay constant $f_\pi = 132$ MeV, and the pion field

$$\hat{\pi} = \begin{pmatrix} \frac{\pi^0}{\sqrt{2}} & \pi^+ \\ \pi^- & -\frac{\pi^0}{\sqrt{2}} \end{pmatrix}. \quad (5)$$

The vector-meson field ρ_μ (for ρ and ω mesons) and the field tensor $F_{\mu\nu}(\rho)$ are given by

$$\rho_\mu = i \frac{g_V}{\sqrt{2}} \hat{\rho}_\mu, \quad (6)$$

$$\hat{\rho}_\mu = \begin{pmatrix} \frac{\rho^0}{\sqrt{2}} + \frac{\omega}{\sqrt{2}} & \rho^+ \\ \rho^- & \frac{-\rho^0}{\sqrt{2}} + \frac{\omega}{\sqrt{2}} \end{pmatrix}_\mu, \quad (7)$$

$$F_{\mu\nu}(\rho) = \partial_\mu \rho_\nu - \partial_\nu \rho_\mu + [\rho_\mu, \rho_\nu], \quad (8)$$

where $g_V = m_V/f_\pi$ is the gauge-coupling constant of the hidden local symmetry [56].

The coupling constant g_π in Eq. (1) is determined by the $D^* \rightarrow D\pi$ decay [49, 50, 57]. For the vector mesons in Eq. (2), β and λ are fixed by radial decays of D^* and semileptonic decays of B with vector-meson dominance [58]. The values of the coupling constants are summarized in Table 1.

The effective Lagrangians for the interaction vertices of nucleons and light mesons are given by

$$\mathcal{L}_{\pi NN} = \sqrt{2} i g_{\pi NN} \bar{N} \gamma_5 \hat{\pi} N, \quad (9)$$

$$\mathcal{L}_{v NN} = \sqrt{2} g_{v NN} \left[\bar{N} \gamma_\mu \hat{\rho}^\mu N + \frac{\kappa}{2m_N} \bar{N} \sigma_{\mu\nu} \partial^\nu \hat{\rho}^\mu N \right], \quad (10)$$

as shown in Refs. [59, 60]. The nucleon field is expressed by $N = (p, n)^t$. The coupling constants, $g_{\pi NN}$, $g_{v NN}$ and κ , are summarized in Table 1.

Table 1 Masses of light mesons $\alpha(=\pi, \rho, \omega)$, m_α , and coupling constants of the Lagrangians. m_α and λ are given in units of MeV and GeV^{-1} , respectively. The other parameters are dimensionless constants.

α	m_α [MeV]	g_π	β	λ [GeV^{-1}]	$g_{\alpha NN}^2/4\pi$	κ
π	132.7	0.59	—	—	13.6	—
ρ	769.9	—	0.9	0.56	0.84	6.1
ω	781.94	—	0.9	0.56	20.0	0.0

In order to parameterize the internal structure of hadrons, the dipole form factor is introduced at each vertex:

$$F_\alpha(\Lambda, \vec{q}) = \frac{\Lambda^2 - m_\alpha^2}{\Lambda^2 + |\vec{q}|^2}, \quad (11)$$

with the mass m_α and the three-momentum \vec{q} of incoming light mesons $\alpha = \pi, \rho, \omega$. As discussed in Refs. [45–47], the cutoff parameter $\Lambda = \Lambda_N$ for the nucleon vertex is determined to reproduce the binding energy of a deuteron. $\Lambda = \Lambda_P$ for the heavy-meson vertex is fixed by the ratio of the sizes of the pseudoscalar (vector) meson $P^{(*)}$ and the nucleon. We use $\Lambda_N = 846$ MeV for the nucleon, $\Lambda_{D^{(*)}} = 1.35\Lambda_N$ for the $\bar{D}^{(*)}$ meson and $\Lambda_{B^{(*)}} = 1.29\Lambda_N$ for the $B^{(*)}$ meson in Refs. [45–47].

From the effective Lagrangians in Eqs. (1)-(10) and the form factor in Eq. (11), the meson exchange potential between a $P^{(*)}$ meson and a nucleon N is obtained. The one-pion exchange potential (OPEP) is expressed by

$$V_{PN-P^*N}^\pi(r) = -\frac{g_\pi g_{\pi NN}}{\sqrt{2}m_N f_\pi} \frac{1}{3} \left[\vec{\varepsilon}^{\prime\dagger} \cdot \vec{\sigma} C(r; m_\pi) + S_\varepsilon T(r; m_\pi) \right] \vec{\tau}_P \cdot \vec{\tau}_N, \quad (12)$$

$$V_{P^*N-P^*N}^\pi(r) = \frac{g_\pi g_{\pi NN}}{\sqrt{2}m_N f_\pi} \frac{1}{3} \left[\vec{S} \cdot \vec{\sigma} C(r; m_\pi) + S_S T(r; m_\pi) \right] \vec{\tau}_P \cdot \vec{\tau}_N, \quad (13)$$

with r being the distance between $P^{(*)}$ and N . $m_N = 940$ MeV is the mass of a nucleon. $\vec{\varepsilon}$ ($\vec{\varepsilon}^\dagger$) is the polarization vector of the incoming (outgoing) heavy vector meson P^* . \vec{S} is the spin-one operator given by $\vec{S} = i\vec{\varepsilon}^\dagger \times \vec{\varepsilon}$. $\vec{\sigma}$ ($\vec{\tau}$) are the Pauli matrices for the (iso)spin. $S_{\mathcal{O}}(\hat{r})$ is the tensor operator expressed by $S_{\mathcal{O}}(\hat{r}) = 3(\vec{\mathcal{O}} \cdot \hat{r})(\vec{\sigma} \cdot \hat{r}) - \vec{\mathcal{O}} \cdot \vec{\sigma}$ for $\mathcal{O} = \varepsilon, S$. The functions $C(r; m_\alpha)$ and $T(r; m_\alpha)$ are given by

$$C(r; m_\alpha) = \int \frac{d^3q}{(2\pi)^3} \frac{m_\alpha^2}{\vec{q}^2 + m_\alpha^2} e^{i\vec{q} \cdot \vec{r}} F(\Lambda_P, \vec{q}) F(\Lambda_N, \vec{q}), \quad (14)$$

$$S_{\mathcal{O}}(\hat{r})T(r; m_\alpha) = \int \frac{d^3q}{(2\pi)^3} \frac{-\vec{q}^2}{\vec{q}^2 + m_\alpha^2} S_{\mathcal{O}}(\hat{q}) e^{i\vec{q} \cdot \vec{r}} F(\Lambda_P, \vec{q}) F(\Lambda_N, \vec{q}). \quad (15)$$

Similarly, the vector-meson exchange potentials are given by

$$V_{PN-PN}^v(r) = \frac{\beta g_V g_{vNN}}{\sqrt{2}m_v^2} C(r; m_v) \vec{\tau}_P \cdot \vec{\tau}_N, \quad (16)$$

$$V_{PN-P^*N}^v(r) = \frac{g_V g_{vNN} \lambda(1 + \kappa)}{\sqrt{2}m_N} \frac{1}{3} [-2\vec{\varepsilon} \cdot \vec{\sigma} C(r; m_v) + S_\varepsilon T(r; m_v)] \vec{\tau}_P \cdot \vec{\tau}_N, \quad (17)$$

$$V_{P^*N-P^*N}^v(r) = \frac{\beta g_V g_{vNN}}{\sqrt{2}m_v^2} C(r; m_v) \vec{\tau}_P \cdot \vec{\tau}_N \\ + \frac{g_V g_{vNN} \lambda(1 + \kappa)}{\sqrt{2}m_N} \frac{1}{3} [2\vec{S} \cdot \vec{\sigma} C(r; m_v) - S_S T(r; m_v)] \vec{\tau}_P \cdot \vec{\tau}_N. \quad (18)$$

The $P^{(*)}N$ potential in the $I(J^P) = 0(1/2^-)$ state is presented by the 3×3 matrix form. The Schrödinger equation is given by

$$\begin{pmatrix} K_0 + V_{11} & V_{12} & V_{13} \\ V_{12} & K_0 + V_{22} & V_{23} \\ V_{13} & V_{23} & K_2 + V_{33} \end{pmatrix} \begin{pmatrix} \psi_1^E \\ \psi_2^E \\ \psi_3^E \end{pmatrix} = E \begin{pmatrix} \psi_1^E \\ \psi_2^E \\ \psi_3^E \end{pmatrix}, \quad (19)$$

with the kinetic term K_ℓ with angular momentum ℓ . The channels $i = 1, 2, 3$ correspond to $PN(^2S_{1/2})$, $P^*N(^2S_{1/2})$ and $P^*N(^4D_{1/2})$, respectively. The potential $V_{ij}(r)$ is the sum of the π , ρ , ω potentials. The explicit forms of the matrix elements as well as the kinetic terms are given in the appendix in Ref. [46]. As shown in Ref. [46], from Eq. (19), we obtain the eigenvalues $E = 2.14$ MeV for the $\bar{D}N$ bound state and 23.04 MeV for the BN bound state.

Let us comment on the interaction employed in this study. We obtain cutoff parameters that are close to the vector-meson masses, and hence the form factor (11) would suppress the contribution from the short-range interaction as the vector-meson exchanges. However, we consider that this short-range interaction includes not only the vector-meson exchange contribution, but also others: the scalar-meson exchange, the η exchange, the $\pi\pi$ exchange, etc. In Refs. [45, 46], we employ the $\pi\rho\omega$ potentials as the nucleon-nucleon interaction, while various short-range interactions can work, as shown in Refs. [59, 60]. Then, the cutoffs of the $\pi\rho\omega$ potentials can be determined as $\Lambda_N = 846$ MeV to reproduce the deuteron properties. In this parameter fitting, the small contribution from the vector-meson exchanges is interpreted as the cancellation of the various short-range interactions with each other. In particular, the scalar-meson exchange provides a strong attraction, and it can suppress the repulsion of the vector-meson exchange potential, as seen in the Bonn potential [59, 60]. The potential employed in this study is also considered to include various meson exchanges, because the cutoffs fixed in the deuteron are used to determine the cutoffs at vertices of the heavy meson and nucleon. Therefore, our vector-meson exchange potential is not pure, but we regard it as a potential including various short-range contributions.

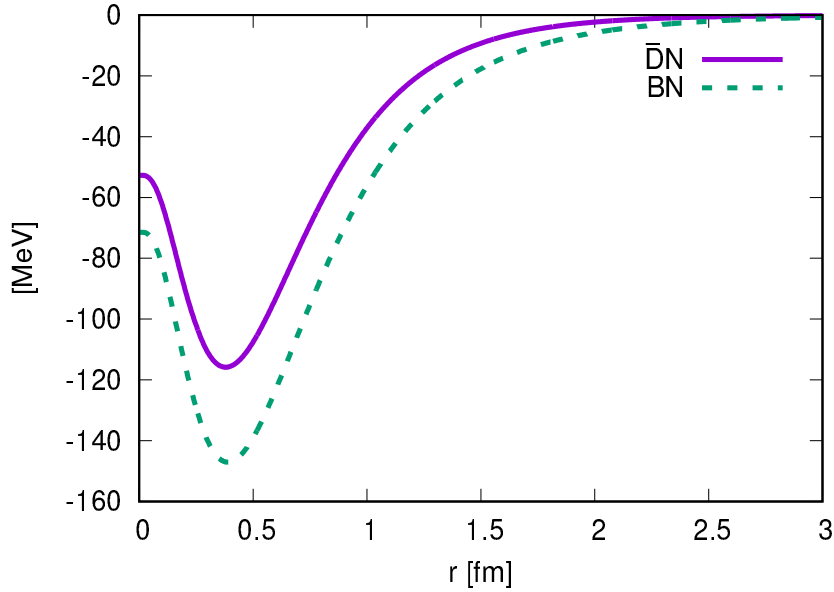


Fig. 1 The single-channel $\bar{D}N$ and BN potentials. The $\bar{D}N$ (BN) potential is plotted by the solid (dashed) line.

2.2 Folding potential

We focus on the $I(J^P) = 0(1/2^-)$ state as the most attractive one, with three channels $PN(^2S_{1/2})$, $P^*N(^2S_{1/2})$, and $P^*N(^4D_{1/2})$. To construct the folding potential between the P meson and the nucleus, we project the $PN - P^*N$ coupled-channel potential onto the PN single-channel potential.

The projection onto the $PN(^2S_{1/2})$ channel is performed by

$$V_{\text{pro}}(r) = V_{11}(r) + V_{12}(r) \frac{\psi_2^E}{\psi_1^E} + V_{13}(r) \frac{\psi_3^E}{\psi_1^E}, \quad (20)$$

with ψ_i^E ($i = 1, 2, 3$) in the coupled-channel Schrödinger equation of the $P^{(*)}N$ two-body system (19). Here E is the binding energy for PN . Then, the single-channel PN potential is obtained as shown in Fig. 1. We notice that $V_{\text{pro}}(r)$ is the energy-dependent potential by its definition. However, in what follows, we assume that $V_{\text{pro}}(r)$ does not qualitatively change so much for different E at normal nuclear matter density, and try to investigate the energy levels of a \bar{D} (B) meson in atomic nuclei.

For the atomic nuclei with $A \gtrsim 16$ (A is the nucleon number), the nucleon number distribution function is approximately expressed by the Woods-Saxon function as

$$\rho(r) = \frac{\rho_0}{1 + \exp((r - R)/a)}, \quad (21)$$

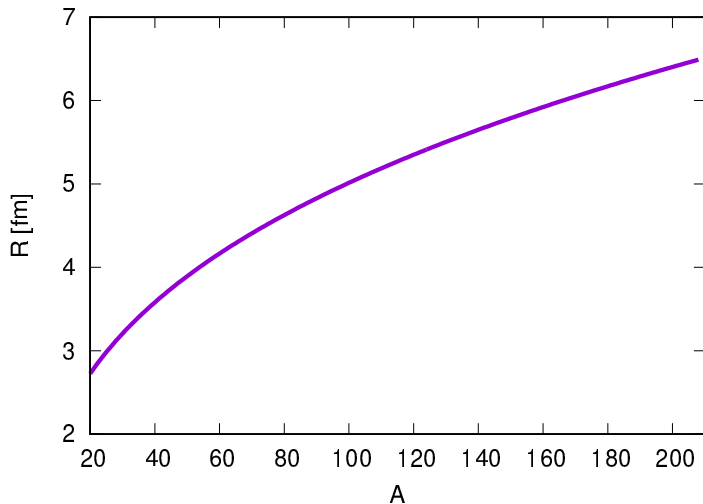


Fig. 2 Nucleon number (A) dependence of R determined by Eq. (22).

where $\rho_0 = 0.17 \text{ fm}^{-3}$ and $a = 0.54 \text{ fm}$ [61]³. r is the distance from the center of the nucleus, and R is determined to satisfy

$$\int \rho(r) d^3r = A. \quad (22)$$

R as a function of $A = 20, \dots, 208$ is shown in Fig. 2. The nucleon number distribution functions for several A are displayed in Fig. 3.

From the single-channel potential in Eq. (20) and the nucleon number distribution function in Eq. (21), the folding potential between the P meson and the nucleus is obtained by

$$V_{\text{fold}}(r) = \int V_{\text{pro}}(r - r') \rho(r') d^3r'. \quad (23)$$

The obtained folding potentials of the \bar{D} (B) meson are shown in Fig. 4.

In this study, we employ the folding potential, which is interpreted as the Hartree potential with the local density approximation. In Eq. (23), V_{pro} corresponds to the Born term of the full t -matrix of the $\bar{D}N$ scattering. In the literature, as the standard approach to obtain the optical potential, the $t\rho$ approximation has been used [62, 63]. If the t -matrix has any pole, however, the breaking down of the $t\rho$ approximation can occur, as was presented in detail in Ref. [16].

³For nuclei with $A < 16$, other shapes of the distribution have been applied, such as a Gaussian function.

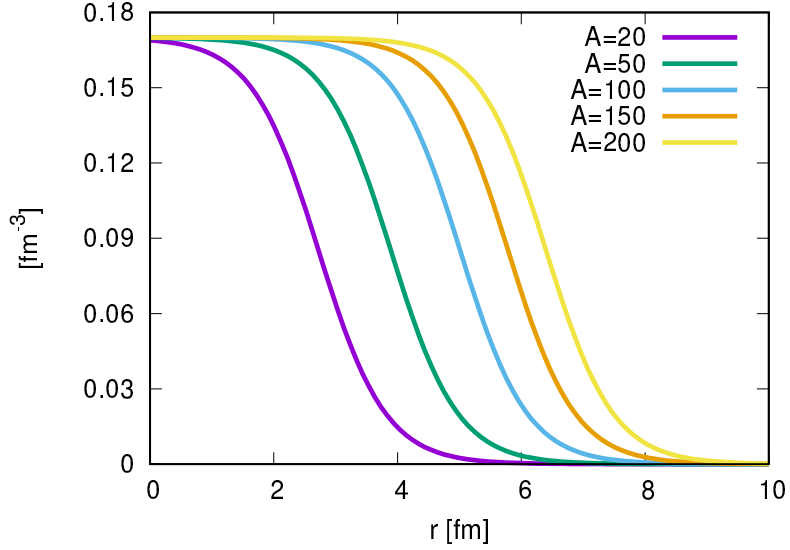


Fig. 3 Nucleon number distribution functions with various nucleon numbers. From left to right, the distributions for $A = 20, 50, 100, 150,$ and 200 are shown.

Let us make a comment on the $I(J^P) = 1(1/2^-)$ channel. The interaction of this channel is repulsive as we obtained a repulsive scattering length, $a_{I=1} = -0.07$ fm, in Ref. [1]. Based on this value, applying the $t\rho$ approximation in Eq. (4.1.24) in Ref. [1], we estimate the mass shift (attraction or repulsion) at normal nuclear matter density, and obtain a positive mass shift by 4 MeV. However, this mass shift is smaller than the potential depth of about 100 MeV (potential value at $r = 0$) for $\bar{D}N$ in $I = 0$ in Fig. 4. Therefore, we may approximately neglect the contribution from $I = 1$ in the present research.

3 Numerical results

From the folding potential in Eq. (23), the binding energies of the P -nucleus systems are obtained by solving the Schrödinger equation for the P meson and the nucleus,

$$-\frac{1}{2\mu} \left(\frac{\partial^2}{\partial r^2} + \frac{2}{r} \frac{\partial}{\partial r} - \frac{\ell(\ell+1)}{r^2} \right) \psi(r) + V_{\text{fold}}(r)\psi(r) = E\psi(r), \quad (24)$$

where the reduced mass μ is given by

$$\frac{1}{\mu} = \frac{1}{m_P} + \frac{1}{Am_N}, \quad (25)$$

with the P meson (nucleon) mass m_P (m_N) and the nucleon number $A = 16, \dots, 208$. ℓ is the relative orbital angular momentum between the P meson and the nucleus.

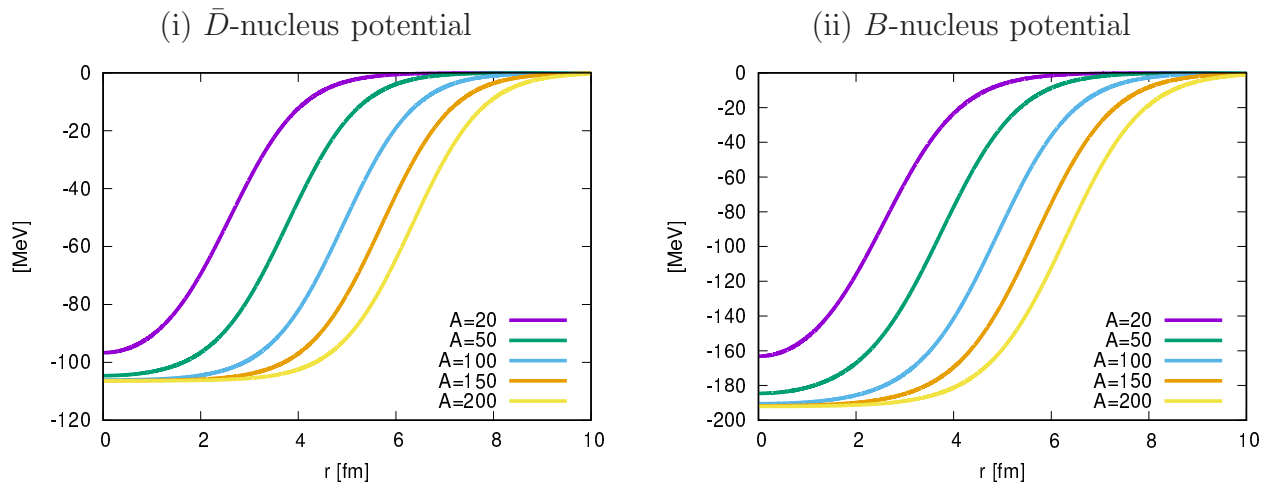


Fig. 4 The folding potentials for the (i) \bar{D} -nucleus and (ii) B -nucleus systems. From left to right, the potentials for $A = 20, 50, 100, 150$ and 200 are shown.

The Schrödinger equation (24) is solved numerically by using the renormalized Numerov method, which was developed in Refs. [64, 65]. We investigate not only a bound state but also a resonance state from a phase shift δ . The resonance energy E_{re} is determined by an inflection point of δ [47, 66], and the decay width is given by $\Gamma = 2/(d\delta/dE)_{E=E_{\text{re}}}$.

The energies are computed for $\ell = 0, 1, 2, 3$, namely S, P, D , and F -waves. For the charm sector, the energies obtained are shown in Fig. 5 for $A = 16$ which is the minimal A to apply Eq. (21), and Fig. 6 with various nucleon numbers for $A = 20, \dots, 208$. The energies of the bottom sector are shown in Figs. 7 and 8 for $A = 16$ and $A = 20, \dots, 208$, respectively.

For the charm sector, we find bound states for the S, P, D , and F -wave states, as shown in Figs. 5 and 6. We emphasize that these bound states are stable against the strong decay. For the S -wave state, three bound states (ground and the first and second excited states) are obtained in $A = 16$. As seen in Fig. 6, the number of bound states increases when the nucleon number increases. Finally, seven bound states are obtained in $A = 208$. The binding energy also increases as A increases. However, the binding energies with respect to A become saturated in the large- A region, because the nucleon number distribution also becomes saturated and the A dependence of the reduced mass (25) becomes smaller. Therefore, the A dependence on the binding energies is flat in the large- A region.

For the states with $\ell \neq 0$, the number of bound states and the values of the binding energy are reduced in comparison with those of $\ell = 0$. As a new phenomenon, resonant states appear slightly above the thresholds. The properties of the resonances are summarized in Table 2.

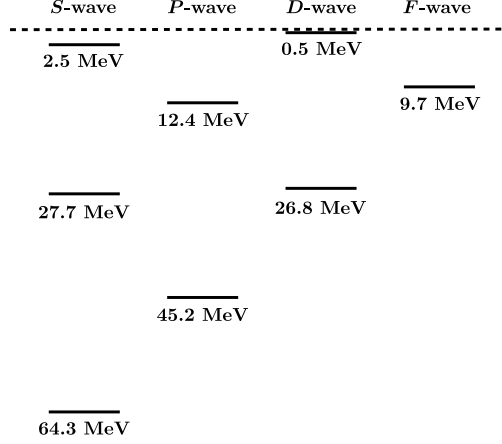


Fig. 5 Energy levels of \bar{D} -nucleus systems with S , P , D , and F -waves for $A = 16$. The solid lines are the energy levels obtained. The values are the binding energies. The dashed line is the threshold.

Table 2 Resonance energy E_{re} and half-decay width $\Gamma/2$ for the \bar{D} -nucleus systems with P , D , and F -waves. E_{re} and $\Gamma/2$ are given in units of MeV.

ℓ	A	E_{re} [MeV]	$\Gamma/2$ [MeV]
P -wave	20	8.90×10^{-2}	3.47×10^{-2}
	40	5.40×10^{-2}	2.02×10^{-2}
D -wave	30	4.82×10^{-1}	7.20×10^{-2}
	160	1.05×10^{-1}	8.40×10^{-3}
F -wave	20	3.29	8.09×10^{-1}
	40	1.95	4.35×10^{-1}
	70	1.85	7.53×10^{-1}
	120	1.23	4.13×10^{-1}
	130	1.85×10^{-1}	1.42×10^{-3}
	190	9.77×10^{-1}	4.46×10^{-1}
	200	3.59×10^{-1}	2.71×10^{-2}

Interestingly, sharp resonances with small widths less than 1 MeV are found. In particular, the F -wave states have many resonances.

For the bottom sector, the attraction of the B -nucleus potential is stronger than the \bar{D} -nucleus one. This is because the mass difference between B and B^* is smaller in the original potential and the strong mixing between BN and B^*N channels induces the stronger

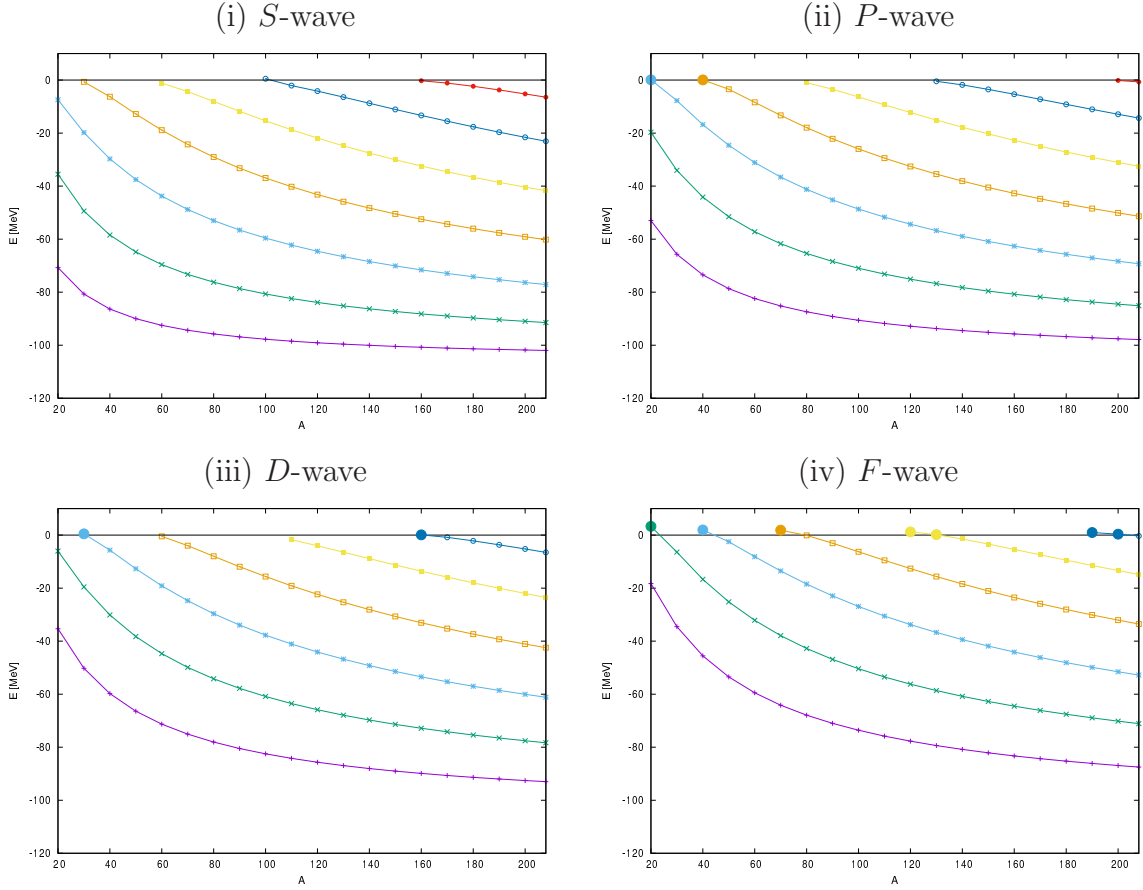


Fig. 6 Nucleon number A dependence on the binding energies of the \bar{D} -nucleus systems with (i) S -wave, (ii) P -wave, (iii) D -wave, and (iv) F -wave. The large filled circle shows resonances. The energy is measured from the \bar{D} -nucleus threshold, and given in units of MeV.

attraction [45–47]. Therefore, more bound states are found. For the S -wave state, the number of bound states is six in $A = 16$ in Fig. 7. In $A = 208$, sixteen states appear as shown in Fig. 8, and the binding energy of the ground state reaches 188.9 MeV. The behavior of the binding energy with respect to A is similar to the \bar{D} -nucleus systems. For $\ell \neq 0$, we find the resonant states that are summarized in Table 3. The B -nucleus systems produce many resonances with small widths.

The wave functions obtained for the \bar{D} , B mesons and the nucleon number distribution function $\rho(r)$ are plotted for $A = 20, 100, 200$ in Fig. 9. The wave functions of the \bar{D} , B mesons are localized inside the nuclei. The wave function of the B -nucleus shrinks more than that of the \bar{D} -nucleus because of the stronger attraction for the former. As the nucleon

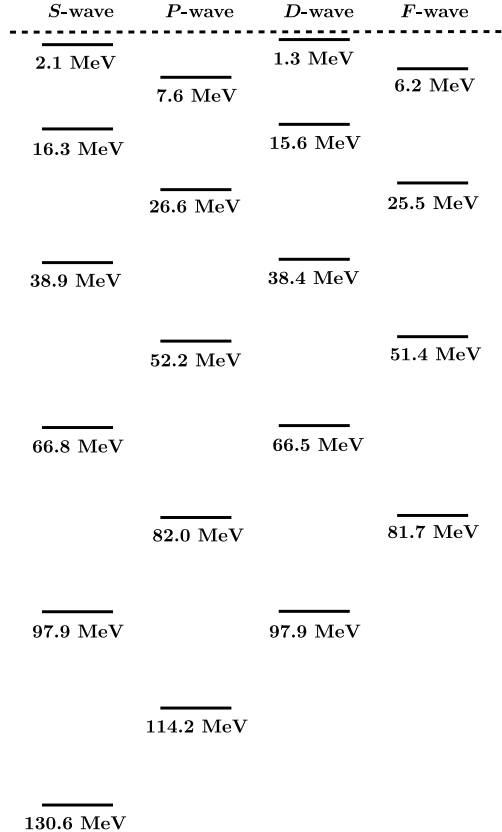


Fig. 7 Energy levels of B -nucleus systems with S , P , D , and F -waves for $A = 16$. The solid lines are the energy levels obtained. The values are the binding energies. The dashed line is the threshold.

number increases, the radii of the nuclei become larger, and accordingly the wave functions of the \bar{D} , B mesons become extended.

For discussion, we compare our results with those in Ref. [16]. First of all, we notice that the interaction between a \bar{D} -meson and a nucleon in Ref. [16] was obtained with a vector-meson exchange model with flavor-spin $SU(8)$ symmetry. The exchanged mesons as well as the method for including the finite-size effect are different from ours. Nevertheless, both results show some similarities. In both cases, there are several excited states from the ground state, and higher angular momentum states are able to exist. As a slight difference, the \bar{D}^0 meson energies in nuclei are saturated at nucleon number $A = 40$ in Ref. [16], while they become saturated for $A \gtrsim 100$ in our analysis. We emphasize that, as a new phenomenon in the present analysis, there exist several resonant states generated by the centrifugal barrier potential near thresholds.

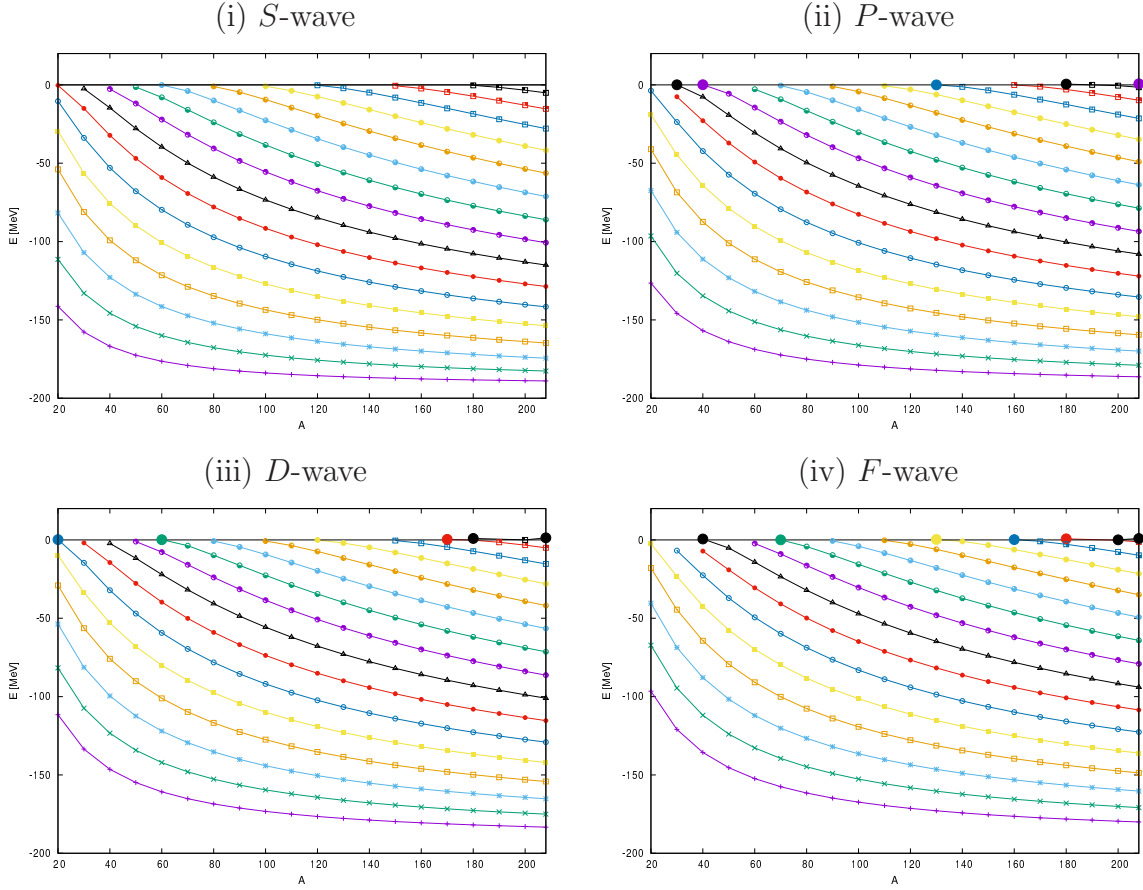


Fig. 8 Nucleon number A dependence on binding energies of the B -nucleus systems with (i) S -wave, (ii) P -wave, (iii) D -wave, and (iv) F -wave. Same convention as Fig. 6.

We also comment that the wave function of the \bar{D} meson in ^{208}Pb was obtained in Ref. [6]. Though the interaction used is different from ours, the wave functions obtained are comparable with ours.

4 Summary

We have studied the bound and resonant systems of the heavy meson ($P = \bar{D}$ or B) and the nucleus with nucleon number $A = 16, \dots, 208$. The attraction between the $P (= \bar{D}, B)$ meson and nucleon N , which is enhanced by the $PN - P^*N$ mixing, inspires us to investigate the stability of exotic heavy mesic nuclei against the strong decay. The mesic nuclei are analyzed as two-body systems of the P meson and the nucleus, where the interaction is described by the folding potential. By using the single-channel PN potential and the nucleon number distribution function, the folding potential is obtained.

Table 3 Resonance energy E_{re} and half-decay width $\Gamma/2$ for the B -nucleus systems with P , D , and F -waves. Same convention as Table 2.

ℓ	A	E_{re} [MeV]	$\Gamma/2$ [MeV]
P -wave	30	4.90×10^{-2}	5.10×10^{-2}
	40	9.30×10^{-3}	2.94×10^{-3}
	130	1.33×10^{-2}	8.00×10^{-3}
	180	4.84×10^{-1}	4.46×10^{-4}
	208	6.94×10^{-1}	1.60×10^{-4}
D -wave	20	2.27×10^{-1}	5.95×10^{-2}
	60	1.38×10^{-1}	4.58×10^{-2}
	170	3.42×10^{-1}	1.25×10^{-2}
	180	9.30×10^{-1}	5.70×10^{-3}
	208	1.36	3.60×10^{-3}
F -wave	40	5.94×10^{-1}	2.76×10^{-1}
	70	3.47×10^{-2}	6.05×10^{-5}
	130	3.21×10^{-1}	1.36×10^{-1}
	160	1.91×10^{-1}	3.76×10^{-2}
	180	7.12×10^{-1}	9.25×10^{-4}
	200	5.96×10^{-2}	1.67×10^{-2}
	208	8.97×10^{-1}	2.72×10^{-4}

We solve the Schrödinger equations of the two-body P -nucleus system with the nucleon number $A = 16, \dots, 208$. Many bound and resonant states are obtained as a result. We find that the binding energy increases as the nucleon number A increases. The A dependence on the binding energy becomes flat in the large- A region.

In the present research, we do not include the possible short-range core in the interaction between a \bar{D} (B) meson and a nucleon. We do not consider the Coulomb potential, which can be important for D^- (B^+) mesons in large nuclei, as discussed in Refs. [6, 16]. It would also be interesting to investigate the D_s^- (B_s^0) mesons in atomic nuclei. Further theoretical discussions are left for future work. The information on the energy spectra of open-heavy mesic nuclear systems will be useful for future experimental research at the Facility for Antiproton and Ion Research (FAIR), the Japan Proton Accelerator Research Complex (J-PARC), the Relativistic Heavy Ion Collider (RHIC), the Large Hadron Collider (LHC), and so forth.

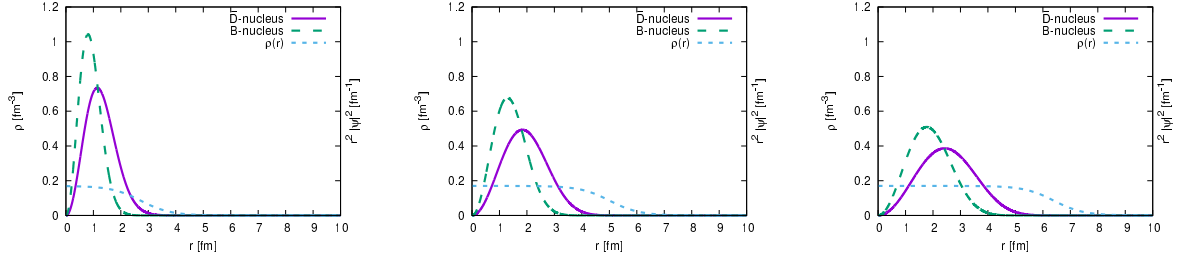


Fig. 9 The wave functions of the ground states with S -wave, $r\psi(r)$, and the nucleon number distribution function, $\rho(r)$, for $A = 20$ (left), $A = 100$ (middle), and $A = 200$ (right). The solid (dashed) lines show $r^2|\psi(r)|^2$ for the \bar{D} -nucleus (the B -nucleus), and the dotted lines show $\rho(r)$.

Acknowledgments

This work is supported in part by the Istituto Nazionale di Fisica Nucleare (INFN) Fellowship Programme and the Special Postdoctoral Researcher (SPDR) Program of RIKEN (Y.Y.). This work is also supported by Grants-in-Aid for Scientific Research (Grant No. 25247036 and No. 15K17641) from the Japan Society for the Promotion of Science (JSPS) (S. Y.).

References

- [1] A. Hosaka, T. Hyodo, K. Sudoh, Y. Yamaguchi, and S. Yasui, Prog. Part. Nucl. Phys. **96**, 88 (2017) [arXiv:1606.08685 [hep-ph]].
- [2] M. Bayar, C. W. Xiao, T. Hyodo, A. Dote, M. Oka, and E. Oset, Phys. Rev. C **86**, 044004 (2012) [arXiv:1205.2275 [hep-ph]].
- [3] A. Yokota, E. Hiyama, and M. Oka, Prog. Theor. Exp. Phys. **2013**, 113D01 (2013) [arXiv:1308.6102 [nucl-th]].
- [4] Y. Yamaguchi, S. Yasui, and A. Hosaka, Nucl. Phys. A **927**, 110 (2014) [arXiv:1309.4324 [nucl-th]].
- [5] S. Maeda, M. Oka, A. Yokota, E. Hiyama, and Y. R. Liu, Prog. Theor. Exp. Phys. **2016**, 023D02 (2016) [arXiv:1509.02445 [nucl-th]].
- [6] K. Tsushima, D. H. Lu, A. W. Thomas, K. Saito, and R. H. Landau, Phys. Rev. C **59**, 2824 (1999) [nucl-th/9810016].
- [7] A. Sibirtsev, K. Tsushima, and A. W. Thomas, Eur. Phys. J. A **6**, 351 (1999) [nucl-th/9904016].
- [8] A. Mishra, E. L. Bratkovskaya, J. Schaffner-Bielich, S. Schramm, and H. Stoecker, Phys. Rev. C **69**, 015202 (2004) [nucl-th/0308082].
- [9] A. Mishra and A. Mazumdar, Phys. Rev. C **79**, 024908 (2009) [arXiv:0810.3067 [nucl-th]].
- [10] A. Kumar and A. Mishra, Phys. Rev. C **81**, 065204 (2010) [arXiv:1005.5018 [nucl-th]].
- [11] A. Kumar and A. Mishra, Eur. Phys. J. A **47**, 164 (2011) [arXiv:1102.4792 [nucl-th]].
- [12] M. F. M. Lutz and C. L. Korpa, Phys. Lett. B **633**, 43 (2006) [nucl-th/0510006].
- [13] T. Mizutani and A. Ramos, Phys. Rev. C **74**, 065201 (2006) [hep-ph/0607257].
- [14] L. Tolos, A. Ramos, and T. Mizutani, Phys. Rev. C **77**, 015207 (2008) [arXiv:0710.2684 [nucl-th]].
- [15] C. E. Jimenez-Tejero, A. Ramos, L. Tolos, and I. Vidana, Phys. Rev. C **84**, 015208 (2011) [arXiv:1102.4786 [hep-ph]].
- [16] C. Garcia-Recio, J. Nieves, L. L. Salcedo, and L. Tolos, Phys. Rev. C **85**, 025203 (2012) [arXiv:1111.6535 [nucl-th]].
- [17] S. Yasui and K. Sudoh, Phys. Rev. C **87**, 015202 (2013). [arXiv:1207.3134 [hep-ph]].
- [18] S. Yasui and K. Sudoh, Phys. Rev. C **89**, 015201 (2014) [arXiv:1308.0098 [hep-ph]].
- [19] A. Hayashigaki, Phys. Lett. B **487**, 96 (2000) [nucl-th/0001051].

- [20] K. Azizi, N. Er, and H. Sundu, *Eur. Phys. J. C* **74**, 3021 (2014) [arXiv:1405.3058 [hep-ph]].
- [21] Z. G. Wang, *Phys. Rev. C* **92**, 065205 (2015) [arXiv:1501.05093 [hep-ph]].
- [22] T. Hilger, R. Thomas, and B. Kampfer, *Phys. Rev. C* **79**, 025202 (2009) [arXiv:0809.4996 [nucl-th]].
- [23] T. Hilger, R. Schulze, and B. Kampfer, *J. Phys. G* **37**, 094054 (2010) [arXiv:1001.0522 [nucl-th]].
- [24] K. Suzuki, P. Gubler and M. Oka, *Phys. Rev. C* **93**, 045209 (2016) [arXiv:1511.04513 [hep-ph]].
- [25] D. Blaschke, P. Costa, and Y. L. Kalinovsky, *Phys. Rev. D* **85**, 034005 (2012) [arXiv:1107.2913 [hep-ph]].
- [26] C. Sasaki, *Phys. Rev. D* **90**, 114007 (2014) [arXiv:1409.3420 [hep-ph]].
- [27] C. Sasaki and K. Redlich, *Phys. Rev. D* **91**, 074021 (2015) [arXiv:1412.7365 [hep-ph]].
- [28] D. Suenaga, B. R. He, Y. L. Ma, and M. Harada, *Phys. Rev. D* **91**, 036001 (2015) [arXiv:1412.2462 [hep-ph]].
- [29] D. Suenaga and M. Harada, *Phys. Rev. D* **93**, 076005 (2016) [arXiv:1509.08578 [hep-ph]].
- [30] S. Yasui and K. Sudoh, *Phys. Rev. C* **88**, 015201 (2013) [arXiv:1301.6830 [hep-ph]].
- [31] S. Yasui, *Phys. Rev. C* **93**, 065204 (2016) [arXiv:1602.00227 [hep-ph]].
- [32] S. Yasui and K. Sudoh, *Phys. Rev. C* **95**, 035204 (2017) [arXiv:1607.07948 [hep-ph]].
- [33] K. Hattori, K. Itakura, S. Ozaki, and S. Yasui, *Phys. Rev. D* **92**, 065003 (2015) [arXiv:1504.07619 [hep-ph]].
- [34] S. Ozaki, K. Itakura, and Y. Kuramoto, *Phys. Rev. D* **94**, 074013 (2016) [arXiv:1509.06966 [hep-ph]].
- [35] S. Yasui, K. Suzuki, and K. Itakura, [arXiv:1604.07208 [hep-ph]].
- [36] S. Yasui, [arXiv:1608.06450 [hep-ph]].
- [37] T. Kanazawa and S. Uchino, *Phys. Rev. D* **94**, 114005 (2016) [arXiv:1609.00033 [cond-mat.str-el]].
- [38] D. Suenaga, B. R. He, Y. L. Ma, and M. Harada, *Phys. Rev. C* **89**, 068201 (2014) [arXiv:1403.5140 [hep-ph]].
- [39] J. Hofmann and M. F. M. Lutz, *Nucl. Phys. A* **763**, 90 (2005) [hep-ph/0507071].
- [40] C. Garcia-Recio, V. K. Magas, T. Mizutani, J. Nieves, A. Ramos, L. L. Salcedo, and L. Tolos, *Phys. Rev. D* **79**, 054004 (2009) [arXiv:0807.2969 [hep-ph]].
- [41] J. Haidenbauer, G. Krein, U. G. Meissner, and A. Sibirtsev, *Eur. Phys. J. A* **33**, 107 (2007) [arXiv:0704.3668 [nucl-th]].
- [42] T. F. Caramés and A. Valcarce, *Phys. Rev. D* **85** 094017 (2012) [arXiv:1204.5502 [hep-ph]].
- [43] T. F. Caramés, C. E. Fontoura, G. Krein, K. Tsushima, J. Vijande, and A. Valcarce, *Phys. Rev. D* **94**, 034009 (2016) [arXiv:1608.04040 [hep-ph]].
- [44] T. D. Cohen, P. M. Hohler, and R. F. Lebed, *Phys. Rev. D* **72**, 074010 (2005) [hep-ph/0508199].
- [45] S. Yasui and K. Sudoh, *Phys. Rev. D* **80**, 034008 (2009) [arXiv:0906.1452 [hep-ph]].
- [46] Y. Yamaguchi, S. Ohkoda, S. Yasui, and A. Hosaka, *Phys. Rev. D* **84**, 014032 (2011) [arXiv:1105.0734 [hep-ph]].
- [47] Y. Yamaguchi, S. Ohkoda, S. Yasui, and A. Hosaka, *Phys. Rev. D* **85**, 054003 (2012) [arXiv:1111.2691 [hep-ph]].
- [48] M. Neubert, *Phys. Rept.* **245**, 259 (1994) [hep-ph/9306320].
- [49] R. Casalbuoni, A. Deandrea, N. Di Bartolomeo, R. Gatto, F. Feruglio, and G. Nardulli, *Phys. Rept.* **281**, 145 (1997) [hep-ph/9605342].
- [50] A. V. Manohar and M. B. Wise, *Heavy Quark Physics* (Cambridge University Press, Cambridge, 2000), Cambridge Monographs on Particle Physics, Nuclear Physics and Cosmology, p.191.
- [51] S. Yasui, K. Sudoh, Y. Yamaguchi, S. Ohkoda, A. Hosaka, and T. Hyodo, *Phys. Lett. B* **727**, 185 (2013) [arXiv:1304.5293 [hep-ph]].
- [52] Y. Yamaguchi, S. Ohkoda, A. Hosaka, T. Hyodo, and S. Yasui, *Phys. Rev. D* **91**, 034034 (2015) [arXiv:1402.5222 [hep-ph]].
- [53] M. B. Wise, *Phys. Rev. D* **45**, R2188 (1992).
- [54] A. F. Falk and M. E. Luke, *Phys. Lett. B* **292**, 119 (1992) [hep-ph/9206241].
- [55] T. M. Yan, H. Y. Cheng, C. Y. Cheung, G. L. Lin, Y. C. Lin, and H. L. Yu, *Phys. Rev. D* **46**, 1148 (1992). Erratum: [*Phys. Rev. D* **55**, 5851 (1997)].
- [56] M. Bando, T. Kugo, and K. Yamawaki, *Phys. Rept.* **164**, 217 (1988).
- [57] C. Patrignani *et al.* [Particle Data Group Collaboration], *Chin. Phys. C* **40**, 100001 (2016).
- [58] C. Isola, M. Ladisa, G. Nardulli, and P. Santorelli, *Phys. Rev. D* **68**, 114001 (2003) [hep-ph/0307367].
- [59] R. Machleidt, K. Holinde, and C. Elster, *Phys. Rept.* **149**, 1 (1987).
- [60] R. Machleidt, *Phys. Rev. C* **63**, 024001 (2001) [nucl-th/0006014].
- [61] A. Bohr and B. R. Mottelson, *Nuclear Structure: Single-Particle Motion/Nuclear Deformations* (World Scientific, Singapore, 1998).
- [62] T. E. O. Ericson and W. Weise, *Pions and Nuclei* (Oxford University Press, Oxford, 1988), The International Series of Monographs on Physics, p. 496.
- [63] R. S. Hayano and T. Hatsuda, *Rev. Mod. Phys.* **82**, 2949 (2010) [arXiv:0812.1702 [nucl-ex]].
- [64] B. R. Johnson, *Chem. Phys.* **67**, 4086 (1977).
- [65] B. R. Johnson, *Chem. Phys.* **69**, 4678 (1978).
- [66] K. Arai and A. T. Kruppa, *Phys. Rev. C* **60**, 064315 (1999).